RSC Advances

PAPER

View Article Online
View Journal | View Issue

Cite this: *RSC Adv.*, 2017, **7**, 31457

Adsorption of H_2S on graphane decorated with Fe, Co and Cu: a DFT study

Qingxiao Zhou, *[ac] Xiangying Su,[a] Weiwei Ju,[a] Yongliang Yong,[a] Xiaohong Li,[a] Zhibing Fu[b] and Chaoyang Wang[b]

Received 2nd May 2017
Accepted 6th June 2017

DOI: 10.1039/c7ra04905f

rsc.li/rsc-advances

Herein, density functional theory (DFT) calculations were performed to investigate the adsorption of a H_2S molecule on the surface of hydrogenated graphene (graphane). In our results, we found that the appearance of an H-vacancy significantly improved the reactivity of graphane due to the unpaired electrons of the vacancy site. However, small adsorption energy and low charge transfer indicated that the interaction between the H_2S molecule and the pure H-vacancy-defected graphane occurred *via* physisorption. By introducing transition-metal dopants (Fe, Co, and Cu), the adsorption process of the H_2S molecule changed to chemisorption. Furthermore, the adsorption of H_2S induced a decrease in the band gaps, which could be seen as signal for the detection of H_2S gas.

1. Introduction

Air pollution is still a global challenge, and daily human and industrial activities are the major source of pollution to the environment, also harming human health. H_2S is a common environmental pollutant, which is usually produced during the preparation process of petroleum and natural gas.[1] It is a highly toxic gas to human beings at low concentrations and can cause mortalities at high concentrations.[2] Hence, the detection of H_2S is a great technological challenge.[3] A promising candidate for gas sensors should possess some advantages such as miniature size, higher sensitivity, and low production cost.[4–6] Recently, graphene, a two-dimensional and one-carbon-thick material, has attracted significant attention due to its excellent physical and chemical properties since its first synthesis was experimentally achieved in 2004.[7–12] Graphene exhibits great promise for the application of gas sensing because it possesses a large surface and high reactivity.[13–17] However, studies suggest that the weak interaction between the adsorbents and graphene and the zero band-gap limit its application in gas detection. To solve this problem, many researchers have focused on improving its reactivity. Several common techniques such as the fictionalization using defects[18–20] and impurities[21–23] have been explored.

Different elements are attached to the surface of graphene to alter its electronic properties and chemical reactivity. Thus, a promising material prepared by exposing graphene to hydrogen plasma is graphane, which was first synthesized in 2009 by Elias *et al.*[24] In graphane, the hydrogen atoms are attached on both sides of graphene, and then, sp^2 hybridization in graphene changes to sp^3 hybridization.[25] Graphane exhibits unique electronic and magnetic properties and has been explored in recent years in the aspects of science and technology, such as transistor and nanoelectronic designs, hydrogen storage, and bio-sensing.[26–31] It is a wide band gap semiconductor and overcomes the restrictions of the non-existence of a band-gap in graphene for some application areas such as gas sensing. Furthermore, its excellent mechanical strength and large surface area predicate its promising application for gas sensing. Islam *et al.*[32] studied the interaction of graphane towards CH_4 molecules, and the results suggested that the H-vacancy and metal-doping significantly enhanced the methane adsorption. Thus, the introduction of an H-vacancy defect and metal-dopants have been successfully attempted to increase the adsorption stability of graphane towards gas molecules.[33–36] In our study, we investigated the adsorption properties of H_2S molecules on the pure, H-vacancy-defected, and transition-metal (TM)-doped graphane using density functional theory (DFT) calculations. The TM-dopants considered herein were Fe, Co, and Cu. We believe that our study provides useful information for the application based on graphane for gas sensing.

2. Computational methods and model

All the DFT calculations were performed *via* the Dmol^3 code.[37] We used the generalized gradient approximation (GGA) for the exchange-correlation functional, as described by Perdew–Burke–Ernzerhof (PBE).[38] Basiuk *et al.* reported that the PBE functional along with Grimme dispersion correction could be

[a]College of Physics and Engineering, Henan University of Science and Technology, Luoyang 471023, People's Republic of China. E-mail: zqxhaust@163.com; Tel: +86 18780539390

[b]Research Center of Laser Fusion, China Academy of Engineering Physics, Mianyang 621900, People's Republic of China

[c]College of Physical Science and Technology, Sichuan University, Chengdu 610065, People's Republic of China

suggested as most suitable for theoretical studies of the interaction between molecules and graphene.[39] Therefore, all the results were obtained using the Grimme-corrected PBE functional. We selected DFT semicore pseudopotential (DSSP) as a single effective potential to replace the core electrons.[40] A double numerical plus polarization (DNP) was employed as the basis set. The DNP basis set corresponded to a double-ζ quality basis set with a p-type polarization function to hydrogen and d-type polarization functions added to heavier atoms, which was comparable with the Gaussian 6-31G (d, p) basis set and exhibited a better accuracy.[41]

We applied a 5 × 5 × 1 supercell under the periodic boundary condition on the x and y axes to model the infinite graphane sheet. The vacuum space of 20 Å was set in the direction normal to the sheets to avoid the interactions between periodic images. A 5 × 5 × 1 mesh of k-point and the global orbital cut-off of 5.0 Å were set in the spin-unrestricted calculations. All atoms were allowed to relax. Convergence in energy, force, and displacement were set at 4.54×10^{-4} eV, 1.09 eV Å^{-1}, and 0.005 Å, respectively.

We analyzed the adsorption of H_2S on hydrogenated graphene (HG). The adsorption energy was obtained from the expression

$$E_{ads} = E(H_2S/HG) - E(HG) - E(H_2S)$$

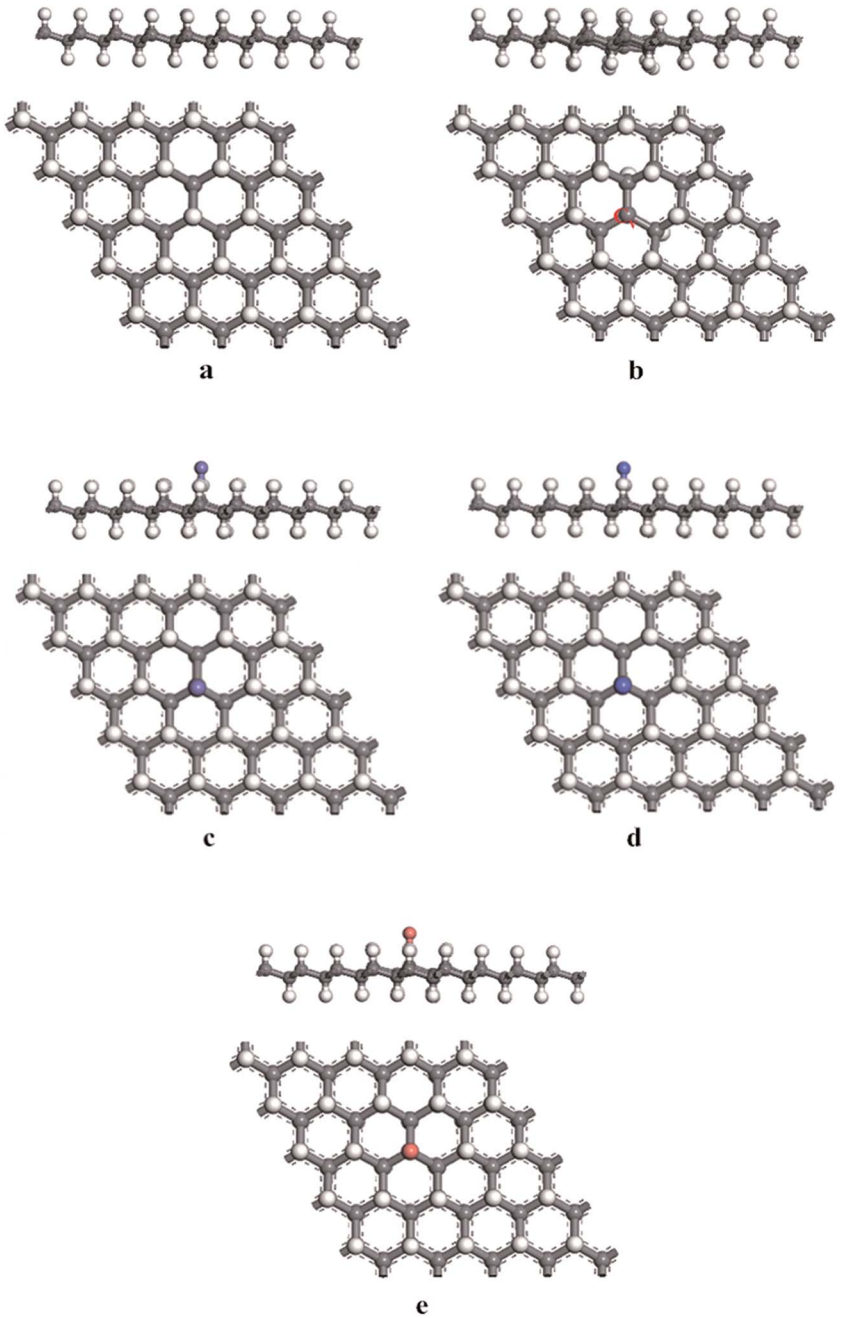

Fig. 1 The optimized structures of (a) HG, (b) VHG, (c) FeVHG, (d) CoVHG, and (e) CuVHG.

where $E(H_2S/HG)$ is the total energy of the H_2S molecule adsorbed on hydrogenated graphene, $E(HG)$ is the total energy of the HG, and $E(H_2S)$ is the total energy of a free H_2S molecule.

3. Results and discussion

3.1 Structures of HG, VHG, FeVHG, CoVHG, and CuVHG

First, we discussed the geometries of pure graphane (HG) and H-vacancy-defected graphane (VHG), and the optimized structures are presented in Fig. 1. The bond lengths of C–H and C–C in the HG configuration were 1.109 Å and 1.496 Å, respectively, which were consistent with those reported in previous studies.[42] Pure graphane was a nonmagnetic semiconductor with a wide gap, which was 3.69 eV as obtained from our calculated results. The gap value was in agreement with the literature, and the little difference was due to the selection of the calculated parameters.[25,42,43] After introducing the H-

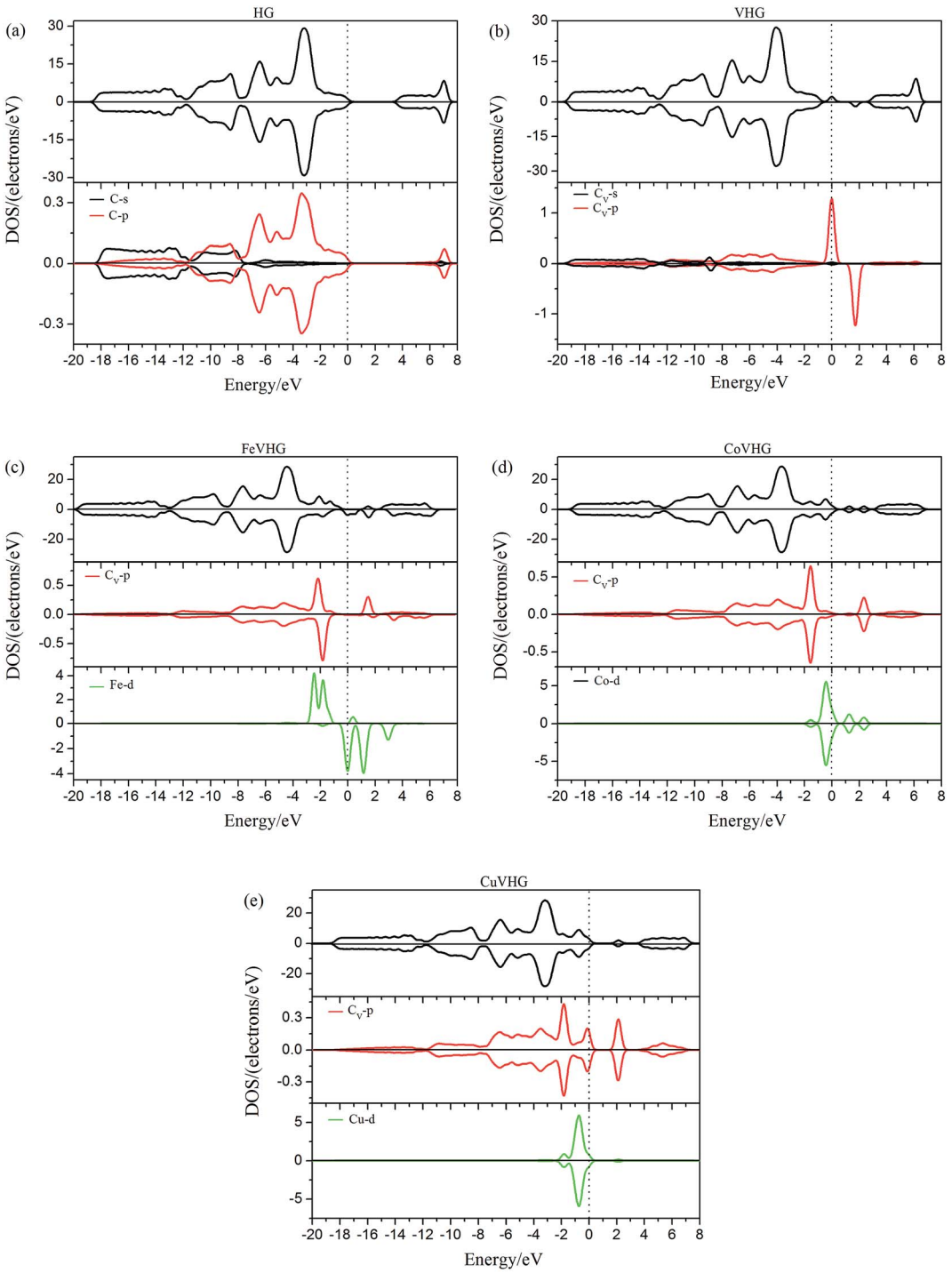

Fig. 2 The PDOS of (a) HG, (b) VHG, (c) FeVHG, (d) CoVHG, and (e) CuVHG.

vacancy defect, the C_v atom, which lost an H atom, was labeled in Fig. 1b. The bond lengths of C_v and the adjacent C atoms were 1.469 Å.

Second, we considered the configuration of VHG doped with Fe (FeVHG), Co (CoVHG), and Cu (CuVHG). Due to the presence of the H-defect in graphane, the vacancy offered a reactive site to craft adsorbents.[35,44] Therefore, we introduced the transition-metal (TM) atoms to the vacancy site. The TM-dopants also preferred to congruously disperse on the graphane surface, which was due to fact that the binding energies were larger than the cohesive energies. The binding energies for the dopants were 3.80 eV, 3.06 eV, and 3.95 eV. Furthermore, the bond lengths of Fe–C_v, Co–C_v, and Cu–C_v were 2.024 Å, 1.977 Å, and 1.967 Å, respectively. The optimized structures were also obtained and are shown in Fig. 1.

To explore the effect of transition-metal dopants on the electronic and magnetic properties of graphane, we performed the density of states (DOS) calculations, as shown in Fig. 2. As shown in Fig. 2a, HG was nonmagnetic and exhibited a wide band gap. However, the H-vacancy released the p electron on the C_v atom and formed a localized state. In our results, VHG exhibited a net magnetic moment of 1 μ_B. As shown in Fig. 2b, the DOS of the C_v-p orbital split into a spin-up and a spin-down peak around the Fermi level, which revealed that the unpaired electrons of C_v induced a half-metallic behavior. Moreover, the band gap of VHG decreased to 1.70 eV. Therefore, VHG was expected to exhibit higher reactivity to interact with the adsorbents as compared to pure graphane.

For the cases of VHG decorated with the TM atoms, there was strong hybridization between the C_v-2p and TM-3d orbitals (Fig. 2c–e). Transition-metal atoms are well known for their magnetic properties. In the case of FeVHG, the Fe-3d orbital exhibited obvious net magnetic moments. For the cases of CoVHG and CuVHG, the magnetic properties disappeared due to the formation of chemical bonds between the dopants and the C_v atoms. In general, the introduction of TM-dopants contributed to the DOS around the Fermi level, and the resulting compounds exhibited higher sensitivity to absorb molecules.

3.2 Adsorption of H_2S on HG and VHG

Herein, we explored the adsorption of H_2S on HG and VHG. According to the geometric symmetry of configuration, there were three initial adsorption structures: the H atom of the H_2S molecule close to the graphane surface with the H–S bond parallel to graphane, the H atom of the H_2S molecule close to the graphane surface with the H–S bond perpendicular to graphane, and the S atom of the H_2S molecule close to the graphane surface. After full relaxation, the calculated results indicated that the S atom of the H_2S molecule close to the graphane was the most stable adsorption structure. We performed the most stable optimized configurations of H_2S/HG and H_2S/VHG, as shown in Fig. 3. Moreover, the corresponding parameters describing the adsorption configurations are summarized in Table 1.

As shown in Table 1, the E_{ads} of H_2S/VHG was −0.05 eV, which was larger than that of H_2S/HG showing a value of −0.02 eV. The enhancement of adsorption stability suggested that the presence of the H-vacancy improved the sensitivity of graphane to absorb the H_2S molecule. The distances between the S atom of the H_2S molecule and the graphane surface (HG and VHG) were 3.299 Å and 4.120 Å, respectively. Moreover, the band gaps of the adsorption complexes were obtained. The E_g of HG and VHG was 3.69 eV and 1.70 eV, which changed to 3.58 eV and 1.66 eV, respectively. The weak interaction with the H_2S molecule did not induce an obvious change in the band gaps of

Table 1 Summary of the results for the H_2S molecule adsorbed on pure graphane (HG) and H-vacancy-defected graphane (VHG). The properties listed are as follows: the distance between the H and S atom of the H_2S molecule (d_{H-S}), the angle of the H_2S molecule (α), the distance between the S atom of H_2S and graphane surface (d_{S-G}), the adsorption energy (E_{ads}), the band gap of the adsorption system (E_g), and the charge transfer of the H_2S molecule (Q)

System	d_{H-S} (Å)	α (°)	d_{S-G} (Å)	E_{ads} (eV)	E_g (eV)	Q (e)
H_2S/HG	1.355⋯1.354	91.44	4.120	−0.02	3.58	0.002
H_2S/VHG	1.355⋯1.356	91.45	3.299	−0.05	1.66	0.007

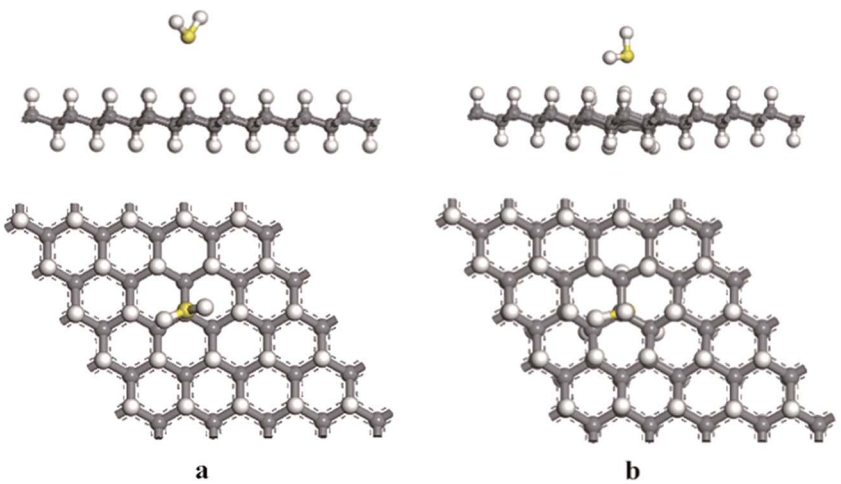

Fig. 3 The optimized structures of (a) H_2S/HG and (b) H_2S/VHG.

the graphane substrate. Moreover, we calculated the charge transfer of the H_2S molecule to graphane. The Q of H_2S/VHG was 0.007 e. The small adsorption energy, large bond distance, and low charge transfer showed that the adsorption of H_2S was due to physisorption.

3.3 Adsorption of H_2S on FeVHG, CoVHG, and CuVHG

Herein, we investigated the adsorption of H_2S on FeVHG, CoVHG, and CuVHG. As stated in Section 3.2, we set the initial adsorption structure with the S atom close to the dopants. After optimization, the adsorption configurations were obtained, as shown in Fig. 4. Furthermore, the corresponding parameters are summarized in Table 2. The adsorption complex of H_2S/CoVHG exhibited maximum stability, of which the adsorption energy was −1.50 eV. Compared with the adsorption of H_2S on HG and VHG, the E_{ads} was enlarged by the introducing of dopants (Fe, Co, and Cu). After interaction with H_2S, the bond lengths of dopant-C_v were elongated such as the d_{C-Fe} changed from 2.224 Å to 2.247 Å. According to the Mulliken analysis results, the Q of H_2S/CoVHG was the highest with the value of 0.302 e. In the adsorption process, the electrons transferred from the H_2S molecule to the graphane substrate. The large adsorption energy and high charge transfer indicated that the introduction of dopants improved the sensitivity to the H_2S molecule and the adsorptions on VHG doped with dopants (Fe, Co, and Cu) were *via* chemisorption.

In our calculated results, the band gaps of FeVHG, CoVHG, and CuVHG were 0.97 eV, 1.26 eV, and 2.33 eV, respectively. The adsorption of the H_2S molecule induced a decrease of band gaps. In the case of H_2S/FeVHG, the E_g was smaller by about 0.2 eV than that of FeVHG. As is well-known, the change in the E_g of the structures induces the electric conductivity change of graphane according to the following equation:[45]

$$\sigma \propto \exp\left(\frac{-E_g}{2kT}\right)$$

where σ is the electric conductivity of the configurations, k is the Boltzmann's constant, and T is the thermodynamic temperature. Therefore, the change of electric conductance of the graphane substrate by the adsorption of the H_2S molecule can be seen as a signal to detect H_2S gas.

3.4 Electronic and magnetic properties

To deeply understand the effect of H-vacancy and dopants on the adsorption of H_2S, we performed the spin polarized density of states (PDOS) of adsorption complexes, as shown in Fig. 5–9. As shown in Fig. 5 and 6, the DOS of H_2S/HG and H_2S/VHG were similar to those of HG and VHG (Fig. 2a and b). From the PDOS of the H_2S molecule, we can see that there was very little interaction between the HG (VHG) sheet and the H_2S molecule.

In the case of H_2S/FeVHG, instead of the two spin-up peaks of the 3d orbital in FeVHG, there was a sharp peak through the Fermi level. Furthermore, we found that a strong hybridization occurred between the Fe-3d and C_v-2p orbitals around the Fermi level, which indicated that a chemical bond formed between the Fe and C_v atoms. For the configuration of H_2S/CoVHG, the spin-up and spin-down of the Co-3d orbitals mismatched and induced a magnetic moment, which resulted from the adsorption of H_2S. There were overlaps between the DOS of Co-3d and S-2p orbitals, which varied from −1.8 eV to −1.5 eV. The strong hybridization explained the strong

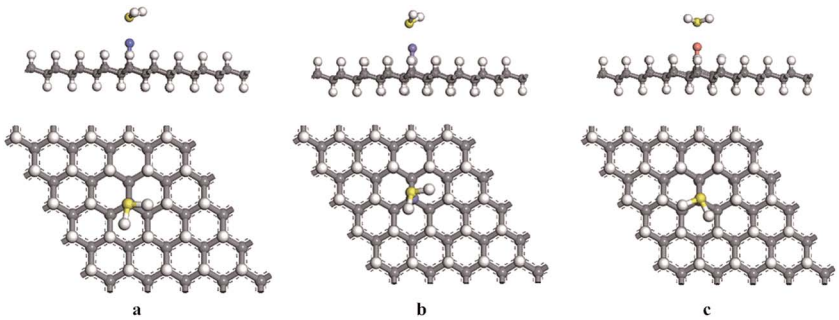

Fig. 4 The optimized structures of (a) H_2S/FeVHG, (b) H_2S/CoVHG, and (c) H_2S/CuVHG.

Table 2 Summary of the results for the H_2S molecule adsorbed on metal atom doped H-vacancy defected graphane. The properties listed are as follows: the distance between the H and S atom of the H_2S molecule (d_{H-S}), the angle of the H_2S molecule (α), the distance between the S atom of H_2S and metal-dopant ($d_{S\text{-dopant}}$), the distance between the C_v atom and metal-dopant ($d_{C\text{-dopant}}$), the adsorption energy (E_{ads}), the band gap of the adsorption system (E_g), and the charge transfer of the H_2S molecule (Q)

System	d_{H-S} (Å)	α (°)	$d_{S\text{-dopant}}$ (Å)	$d_{C\text{-dopant}}$ (Å)	E_{ads} (eV)	E_g (eV)	Q (e)
H_2S/FeVHG	1.370⋯1.371	90.45	2.247	2.047	−0.93	0.75	0.058
H_2S/CoVHG	1.369⋯1.371	90.36	2.221	1.995	−1.50	1.10	0.170
H_2S/CuVHG	1.363⋯1.363	91.71	2.220	1.966	−0.88	2.12	0.302

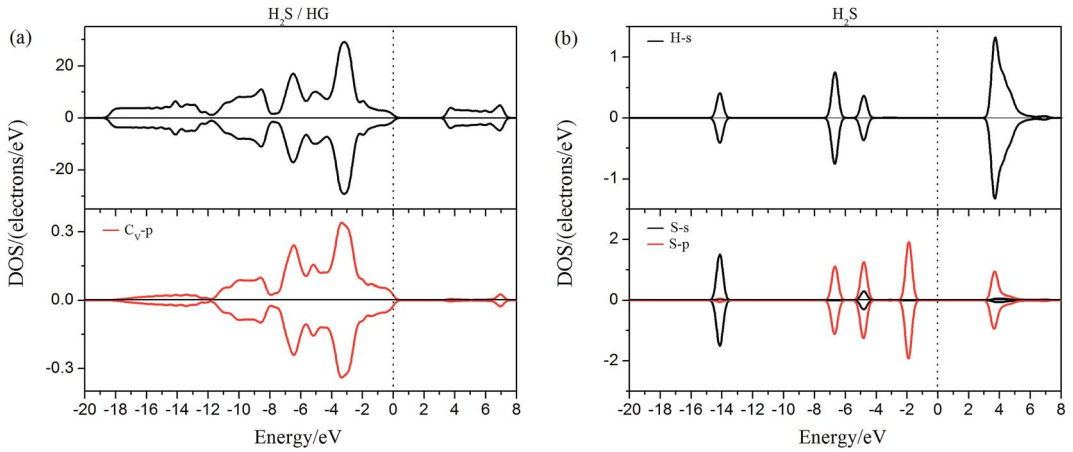

Fig. 5 The PDOS of the (a) H_2S/HG complex and (b) H_2S molecule.

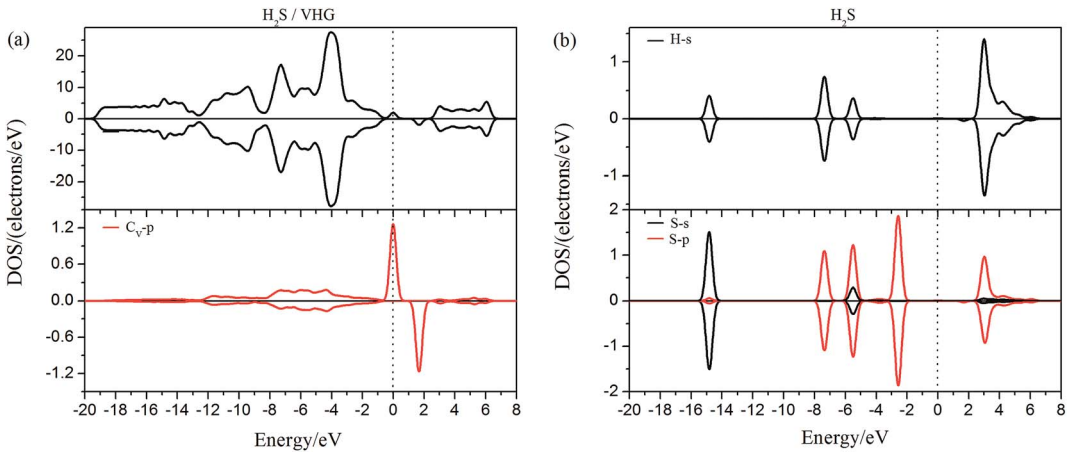

Fig. 6 The PDOS of the (a) H_2S/VHG complex and (b) H_2S molecule.

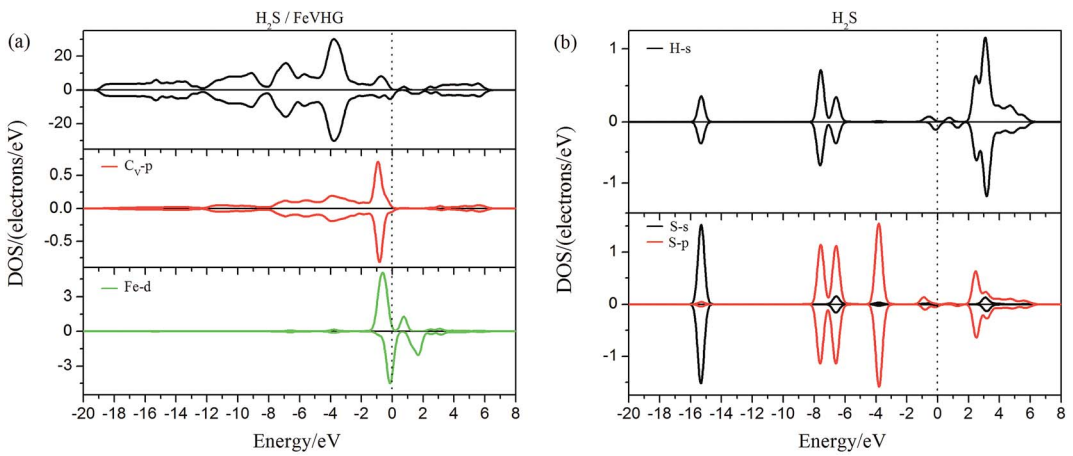

Fig. 7 The PDOS of the (a) H_2S/FeVHG complex and (b) H_2S molecule.

affinity of CoVHG towards the H_2S gas molecule. As above-mentioned, the contribution of the 3d orbital of dopants to the DOS around the Fermi level improved the reactivity of graphane and the strong interaction between the dopants and molecules was responsible for the increase in the adsorption energy.

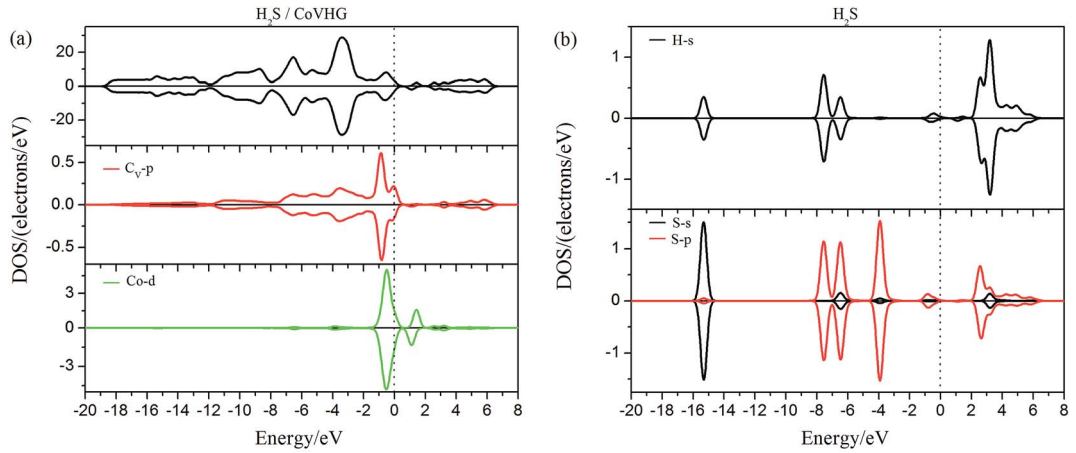

Fig. 8 The PDOS of the (a) H_2S/CoVHG complex and (b) H_2S molecule.

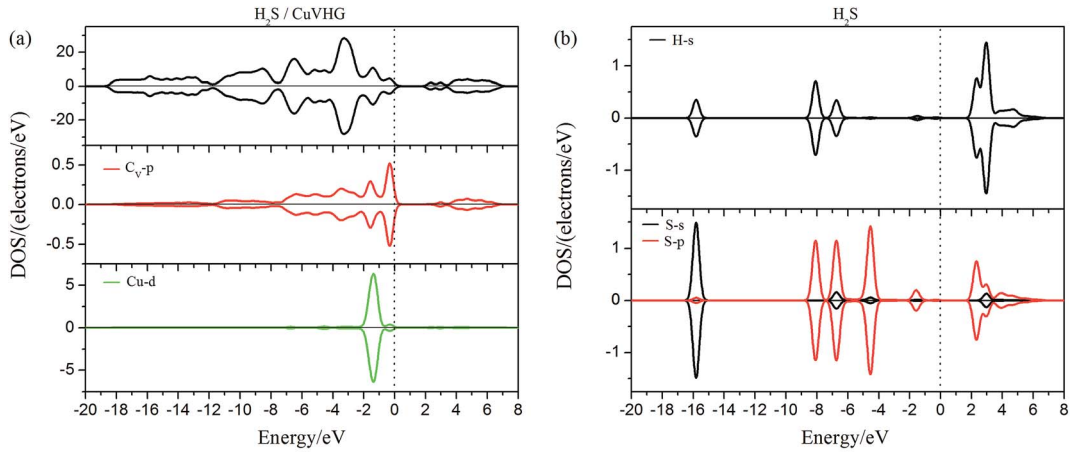

Fig. 9 The PDOS of (a) H_2S/CuVHG complex and (b) H_2S molecule.

4. Conclusions

In summary, we explored the adsorption of the H_2S molecule on the surface of pure graphane, and H-vacancy-defected and transition-metal-doped graphane. First, we investigated the effect of the H-vacancy and dopants on the geometric structure and electronic properties of graphane. Our results revealed that the states of C_v and dopants were available near the Fermi level and improved the reactivity of the graphane substrate. Furthermore, the C_v atom exhibited a half-metallic behavior. Second, we calculated the adsorption energy, bond length, band gap, and charge transfer for the adsorption systems. The results suggested that the H-vacancy and dopants enhanced the adsorption stability of H_2S on the graphane surface. Furthermore, the PDOS results indicated that there was a strong hybridization between the C_v-p orbital and the dopants. Based on these results, it can be concluded that TM-doped graphane is capable of becoming a new sensor for H_2S molecules. We believe that our results can provide useful information towards the applications based on graphane.

Acknowledgements

This work was supported by the National Natural Science Foundation of China (NSFC, Grant No. 11604080, 11404096, U1404609, 11304080, 11547153) and the Innovation Team of Henan University of Science and Technology (No. 2015XTD001).

References

1 H. Kimura, Physiological Role of Hydrogen Sulfide and Polysulfide in the Central Nervous System, *Neurochem. Int.*, 2013, **63**, 492.

2 L. Spadaro, A. Palella, F. Frusteri and F. Arena, Valorization of Crude Bio-Oil to Sustainable Energy Vector for Applications in Cars Powering and on-Board Reformers Via Catalytic Hydrogenation, *Int. J. Hydrogen Energy*, 2015, **40**, 14507–14518.

3 P. P. Hankare, S. D. Jadhav, U. B. Sankpal, R. P. Patil, R. Sasikala and I. S. Mulla, Gas Sensing Properties of Magnesium Ferrite Prepared by Co-Precipitation Method, *J. Alloys Compd.*, 2009, **488**, 270–272.

4 S. Capone, A. Forleo, L. Francioso, R. Rella, P. Siciliano, J. Spadavecchia, D. S. Presicce and A. M. Taurino, Solid State Gas Sensors: State of the Art and Future Activities, *ChemInform*, 2004, **35**, 1335–1348.

5 N. Barsan, D. Koziej and U. Weimar, Metal Oxide-Based Gas Sensor Research: How To?, *Sens. Actuators, B*, 2007, **121**, 18–35.

6 A. Kolmakov and M. Moskovits, Chemical Sensing and Catalysis by One-Dimensional Metal-Oxide Nanostructures, *Annu. Rev. Mater. Res.*, 2004, **35**, 151–180.

7 K. S. Novoselov, A. K. Geim, S. V. Morozov, D. Jiang, Y. Zhang, S. V. Dubonos, I. V. Grigorieva and A. A. Firsov, Electric Field Effect in Atomically Thin Carbon Films, *Science*, 2004, **306**, 666.

8 S. Stankovich, D. A. Dikin, G. H. B. Dommett, K. M. Kohlhaas, E. J. Zimney, E. A. Stach, R. D. Piner, S. T. Nguyen and R. S. Ruoff, Graphene-Based Composite Materials, *Nature*, 2006, **442**, 282–286.

9 J. Gu, C. Liang, X. Zhao, B. Gan, H. Qiu, Y. Guo, X. Yang, Q. Zhang and D. Y. Wang, Highly Thermally Conductive Flame-Retardant Epoxy Nanocomposites with Reduced Ignitability and Excellent Electrical Conductivities, *Compos. Sci. Technol.*, 2017, **139**, 83–89.

10 Q. Zhou, Z. Fu, Y. Tang, H. Zhang and C. Wang, First-Principle Study of the Transition-Metal Adatoms on B-Doped Vacancy-Defected Graphene, *Phys. E*, 2014, **60**, 133–138.

11 R. R. Q. Freitas, R. Rivelino, F. d. B. Mota and C. M. C. de Castilho, Dft Studies of the Interactions of a Graphene Layer with Small Water Aggregates, *J. Phys. Chem. A*, 2011, **115**, 12348–12356.

12 J. Sabio, C. Seoánez, S. Fratini, F. Guinea, A. H. C. Neto and F. Sols, Electrostatic Interactions between Graphene Layers and Their Environment, *Phys. Rev. B: Condens. Matter Mater. Phys.*, 2008, **77**, 195409.

13 B. S. Li, P. W. Yong and K. D. Hai, First-Principle Study of Structural, Electronic, Vibrational and Magnetic Properties of Hcn Adsorbed Graphene Doped with Cr, Mn and Fe, *Appl. Surf. Sci.*, 2015, **329**, 330–336.

14 A. S. Rad, Al-Doped Graphene as a New Nanostructure Adsorbent for Some Halomethane Compounds: Dft Calculations, *Surf. Sci.*, 2016, **645**, 6–12.

15 X. Zhang, L. Yu, Y. Gui and W. Hu, First-Principles Study of Sf 6 Decomposed Gas Adsorbed on Au-Decorated Graphene, *Appl. Surf. Sci.*, 2016, **367**, 259–269.

16 Y. Tang, W. Chen, C. Li, L. Pan, X. Dai and D. Ma, Adsorption Behavior of Co Anchored on Graphene Sheets toward No, So 2, Nh 3, Co and Hcn Molecules, *Appl. Surf. Sci.*, 2015, **342**, 191–199.

17 Y. Tang, Z. Liu, Z. Shen, W. Chen, D. Ma and X. Dai, Adsorption Sensitivity of Metal Atom Decorated Bilayer Graphene toward Toxic Gas Molecules (CO, NO, SO_2 and HCN), *Sens. Actuators, B*, 2016, **238**, 182–195.

18 F. Ding, Theoretical Study of the Stability of Defects in Single-Walled Carbon Nanotubes as a Function of Their Distance from the Nanotube End, *Phys. Rev. B: Condens. Matter Mater. Phys.*, 2005, **72**, 245409.

19 R. M. Ribeiro, N. M. R. Peres, J. Coutinho and P. R. Briddon, Inducing Energy Gaps in Monolayer and Bilayer Graphene: Local Density Approximation Calculations, *Phys. Rev. B: Condens. Matter Mater. Phys.*, 2008, **78**, 075442.

20 S. C. Pradhan and J. K. Phadikar, Small Scale Effect on Vibration of Embedded Multilayered Graphene Sheets Based on Nonlocal Continuum Models, *Phys. Lett. A*, 2009, **373**, 1062–1069.

21 S. Gholami, A. S. Rad, A. Heydarinasab and M. Ardjmand, Adsorption of Adenine on the Surface of Nickel-Decorated Graphene; a DFT Study, *J. Alloys Compd.*, 2016, **686**, 662–668.

22 M. Kunaseth, T. Mudchimo, S. Namuangruk, N. Kungwan, V. Promarak and S. Jungsuttiwong, A Dft Study of Arsine Adsorption on Palladium Doped Graphene: Effects of Palladium Cluster Size, *Appl. Surf. Sci.*, 2016, **367**, 552–558.

23 W. Zan, W. Geng, H. Liu and X. Yao, Influence of Interface Structures on the Properties of Molybdenum Disulfide/Graphene Composites: A Density Functional Theory Study, *J. Alloys Compd.*, 2015, **649**, 961–967.

24 D. C. Elias, R. R. Nair, T. M. G. Mohiuddin, S. V. Morozov, P. Blake, M. P. Halsall, A. C. Ferrari, D. W. Boukhvalov, M. I. Katsnelson and A. K. Geim, Control of Graphene's Properties by Reversible Hydrogenation: Evidence for Graphane, *Science*, 2009, **323**, 610–613.

25 O. Leenaerts, H. Peelaers, A. D. Hernández-Nieves, B. Partoens and F. M. Peeters, First-Principles Investigation of Graphene Fluoride and Graphane, *Phys. Rev. B: Condens. Matter Mater. Phys.*, 2010, **82**, 195436.

26 H. Şahin, C. Ataca and S. Ciraci, Magnetization of Graphane by Dehydrogenation, *Appl. Phys. Lett.*, 2009, **95**, 222510.

27 T. Hussain, B. Pathak, M. Ramzan, T. A. Maark and R. Ahuja, Calcium Doped Graphane as a Hydrogen Storage Material, *Appl. Phys. Lett.*, 2012, **100**, 302–304.

28 S. Haldar, D. G. Kanhere and B. Sanyal, Magnetic Impurities in Graphane with Dehydrogenated Channels, *Phys. Rev. B: Condens. Matter Mater. Phys.*, 2012, **85**, 155426.

29 T. Hussain, A. D. Sarkar and R. Ahuja, Strain Induced Lithium Functionalized Graphane as a High Capacity Hydrogen Storage Material, *Appl. Phys. Lett.*, 2012, **101**, 103907.

30 C. Zhou, S. Chen, J. Lou, J. Wang, Q. Yang, C. Liu, D. Huang and T. Zhu, Graphene's Cousin: The Present and Future of Graphane, *Nanoscale Res. Lett.*, 2014, **9**, 26.

31 R. E. Mapasha, M. P. Molepo and N. Chetty, Ab Initio Studies of Isolated Hydrogen Vacancies in Graphane, *Phys. E*, 2016, **79**, 52–58.

32 M. S. Islam, T. Hussain, G. S. Rao, P. Panigrahi and R. Ahuja, Augmenting the Sensing Aptitude of Hydrogenated Graphene by Crafting with Defects and Dopants, *Sens. Actuators, B*, 2016, **228**, 317–321.

33 J. Berashevich and T. Chakraborty, Influence of Adsorbates on the Electronic and Magnetic Properties of Graphane with H-Vacancy Defects, *Phys. Rev. B: Condens. Matter Mater. Phys.*, 2010, **82**, 134415.

34 C. K. Yang, Graphane with Defect or Transition-Metal Impurity, *Carbon*, 2010, **48**, 3901–3905.

35 T. Hussain, P. Panigrahi and R. Ahuja, Enriching Physisorption of H_2S and NH_3 Gases on a Graphane Sheet by Doping with Li Adatoms, *Phys. Chem. Chem. Phys.*, 2014, **16**, 8100–8105.
36 H. Tanveer, P. Puspamitra and A. Rajeev, Sensing Propensity of a Defected Graphane Sheet Towards CO, H_2O and NO_2, *Nanotechnology*, 2014, **25**, 325501.
37 B. Delley, From Molecules to Solids with the Dmol3 Approach, *J. Chem. Phys.*, 2000, **113**, 7756–7764.
38 J. P. Perdew, K. Burke and M. Ernzerhof, Generalized Gradient Approximation Made Simple, *Phys. Rev. Lett.*, 1996, **77**, 3865–3868.
39 V. A. Basiuk and L. V. Henaoholguín, Dispersion-Corrected Density Functional Theory Calculations of Meso-Tetraphenylporphine-C_{60} Complex by Using $Dmol^3$ Module, *J. Comput. Theor. Nanosci.*, 2014, **11**, 1609–1615.
40 D. J. Chadi, Special Points for Brillouin-Zone Integrations, *Phys. Rev. B: Solid State*, 1976, **13**, 5188–5192.
41 B. Delley, Hardness Conserving Semilocal Pseudopotentials, *Phys. Rev. B: Condens. Matter Mater. Phys.*, 2002, **66**, 155125.
42 J. O. Sofo, A. S. Chaudhari and G. D. Barber, Graphane: A Two-Dimensional Hydrocarbon, *Phys. Rev. B: Condens. Matter Mater. Phys.*, 2007, **75**, 153401.
43 S. Lebègue, M. Klintenberg, O. Eriksson and M. I. Katsnelson, Accurate Electronic Band Gap of Pure and Functionalized Graphane from Gw Calculations, *Phys. Rev. B: Condens. Matter Mater. Phys.*, 2009, **79**, 245117.
44 Y. H. Zhang, Y. B. Chen, K. G. Zhou, C. H. Liu, J. Zeng, H. L. Zhang and Y. Peng, Improving Gas Sensing Properties of Graphene by Introducing Dopants and Defects: A First-Principles Study, *Nanotechnology*, 2009, **20**, 185504.
45 S. S. Li, *Semiconductor Physical Electronics*, Springer, USA, 2nd edn, 2006.